Investigation of Propeller-Induced Tip Vortices Using Particle Image Velocimetry

Abel Viji George[1]
Department of Aerospace Engineering
Indian Institute Of Technology - Madras
Chennai, India
ae21b001@smail.iitm.ac.in

***Abstract*—This study investigates the characteristics of tip vortices generated by 2-bladed and 3-bladed propellers in quiescent flow using particle image velocimetry (PIV). A desktop-scale PIV experiment was designed to capture instantaneous velocity fields, with a focus on vortex evolution, propagation, and dissipation. Results demonstrate that 3-bladed propellers produce vortices that interact more closely and dissipate faster compared to the distinct, long-lived vortices of 2-bladed propellers. Higher rotational speeds amplified vortex generation and longevity, while finite domain boundaries induced reverse flow that suppressed vortex structures. These findings align with noise reduction trends observed in multi-bladed propellers, suggesting that vortex interaction dynamics play a critical role in acoustic performance. The experimental methodology and comparative analysis provide insights for optimizing propeller designs in aerospace and marine applications.**

***Index Terms*—Tip Vortices, Aerodynamic noise, PIV, Dissipation, Convection**

I. Introduction

The demand for energy-efficient and quieter propeller-driven systems in aerial and marine applications has intensified with the rise of urban air mobility, amphibious drones, and sustainable marine transport. Propeller design critically influences both aerodynamic/hydrodynamic performance and acoustic signatures, with blade number emerging as a pivotal parameter. While increasing blade count enhances thrust and torque at a given rotational speed, it introduces complex trade-offs in vortex dynamics and operational efficiency.

Tip vortices, generated at propeller blade tips, are a dominant source of energy loss, vibration, and noise [1]. These coherent structures arise from the pressure differential between the suction and pressure sides of blades, shedding into the wake with rotational kinetic energy. Recent studies confirm that two-bladed propellers produce stronger, more persistent tip vortices compared to multi-bladed configurations, correlating with higher tonal noise levels at equivalent tip speeds [2].

Particle image velocimetry (PIV) has proven indispensable for resolving tip vortex kinematics. Studies have quantified near-wake vorticity and secondary vortex interactions using phase-locked PIV, revealing how viscous effects dominate slipstream broadening beyond one propeller diameter [3]. Expanding on this understanding by employing PIV in cavitation tunnels to track helical tip vortex trajectories, the slipstream contraction in the near wake followed by vortex breakdown due to viscous dissipation has been demonstrated [1]. These experimental insights are critical for validating computational fluid dynamics (CFD) models, which often oversimplify vortex core instabilities and breakdown mechanisms.

While tip vortices are inherently three-dimensional, 2D-2C PIV remains a widely accepted and validated method for capturing key vortex characteristics. 2D-PIV has been applied to quantify vortex core radii, jittering zones, and convection velocities in wind turbine wakes [4]. They demonstrated that vortex identification methods (e.g., vorticity, Q-criterion) reliably extract vortex parameters from 2D data, even with inherent 3D wandering.

Despite advances, not enough work has been done to use PIV measurements to try and link the tip voices and propeller noise, particularly for small-scale propellers in still fluid. This work bridges that gap by employing desktop-scale PIV to analyze tip vortex evolution, interaction, and decay in 2-bladed and 3-bladed propellers under quiescent flow.

II. Methodology

A. Experimental setup

The setup as shown in Figure 1 consists of a glass tank of dimension $26cm \times 17cm \times 19cm$ which is the domain of the experiment. The PIV is carried out in water with hollow glass spheres of approximate diameter $100\mu m$ and density of about $1.1g/cm^3$ as the tracer particles. A green pointer laser of wavelength $532nm$ and maximum power $< 100mW$ is used with a cylindrical lens to generate the laser sheet to illuminate the flow. An industrial two-bladed propeller of diameter $45mm$ and a resin 3D printed three-bladed propeller of the same diameter is used for the experiments. A micro-coreless motor of rating $3.7V$ and $0.8A$ is used for rotating the propellers inside water. The laser-cylindrical lens assembly and the motor-propeller assembly were held at the correct position by using a laboratory stand and clamps.

A Photron UX Mini 50 high speed camera at 500 Hz is used to measure the rpm of the rotating blades at different voltages which is controlled by a voltage regulator. This is necessary as the motor-propeller assembly rotates at different speeds in air and water. A DSLR camera at 100 Hz is used to to capture

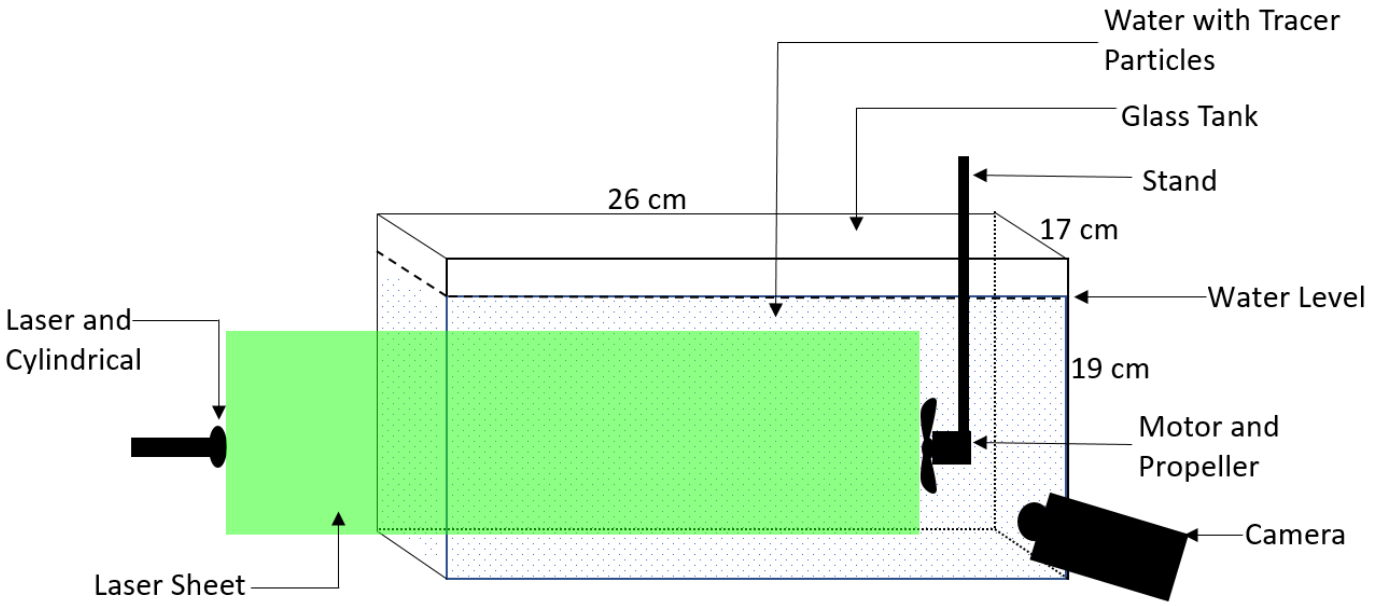

Fig. 1: Sketch of the experimental setup

the PIV images. A tripod stand was used to adjust the position of the camera so that the field of view is sufficient and the tracer particles are in focus.

B. Analysis

Video recordings from the PIV experiments were transferred from the DSLR camera to a laptop with an Intel i5 processor and 8 GB RAM, and all subsequent analyses were carried out on this system using the open-source toolbox PIVLab in Matlab [5], [6]. The videos were converted to distinct frames and the inbuilt PIV cross correlation algorithm is applied on them to obtain the velocity data. The images are calibrated using a calibration image captured along with the setup without changing the camera configurations. This is necessary to accurately quantify the data we obtain. Using the velocity information, all the subsequent analyses like obtaining vorticity field, vortex locators etc. can be calculated.

III. Results

It is known that large aircraft prefer higher number of propeller blades for a larger thrust requirement [2]. Figure 2 shows this trend by computing the static thrust of both the propellers and it becomes more pronounced at higher RPMs.

$$T_{st} = \frac{1}{2}\rho A V_0^2 \tag{1}$$

where, ρ is the density of the fluid, A is the area of the propeller disk and V_0 is the maximum fluid velocity passing through the disk. Note that only a qualitative estimation can be obtained as we are ignoring the efficiency of both the propellers.

It was shown that increasing the number of blades of the propeller resulted in lesser noise generated [7] and resulted in merging of vortices [2]. Figure 3 shows the vortices identified

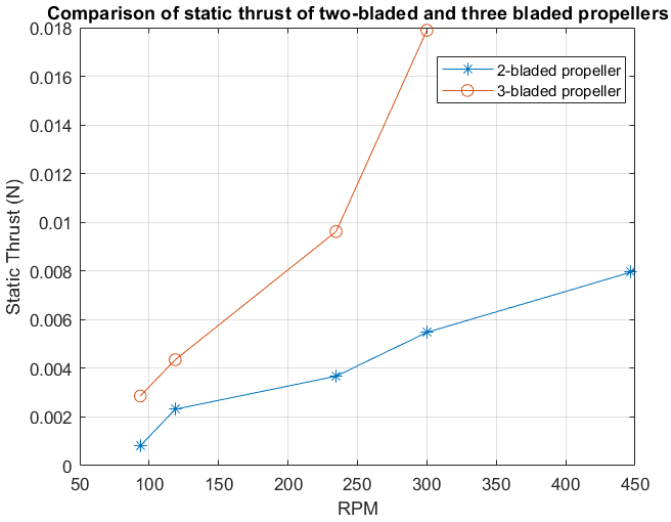

Fig. 2: Comparison of Thrust by varying RPMs for two bladed and three bladed propellers using the relation

through Vortex locators (e.g. through discriminant for complex eigenvalues [8]) applied on the velocity field. The propeller center is at the origin and the x and y locations are non-dimensionalised with the propeller diameter, D.

At the same rotational speed, tip vortices from a two-bladed propeller appear more isolated and coherent, whereas those from a three-bladed propeller are more numerous and closely spaced. The increased proximity promotes vortex–vortex interaction and accelerated dissipation into smaller structures [1], resulting in a finer and more fragmented vortex field with higher blade counts. Additionally, the small propeller diameter brings the blade tips closer to each other and to the

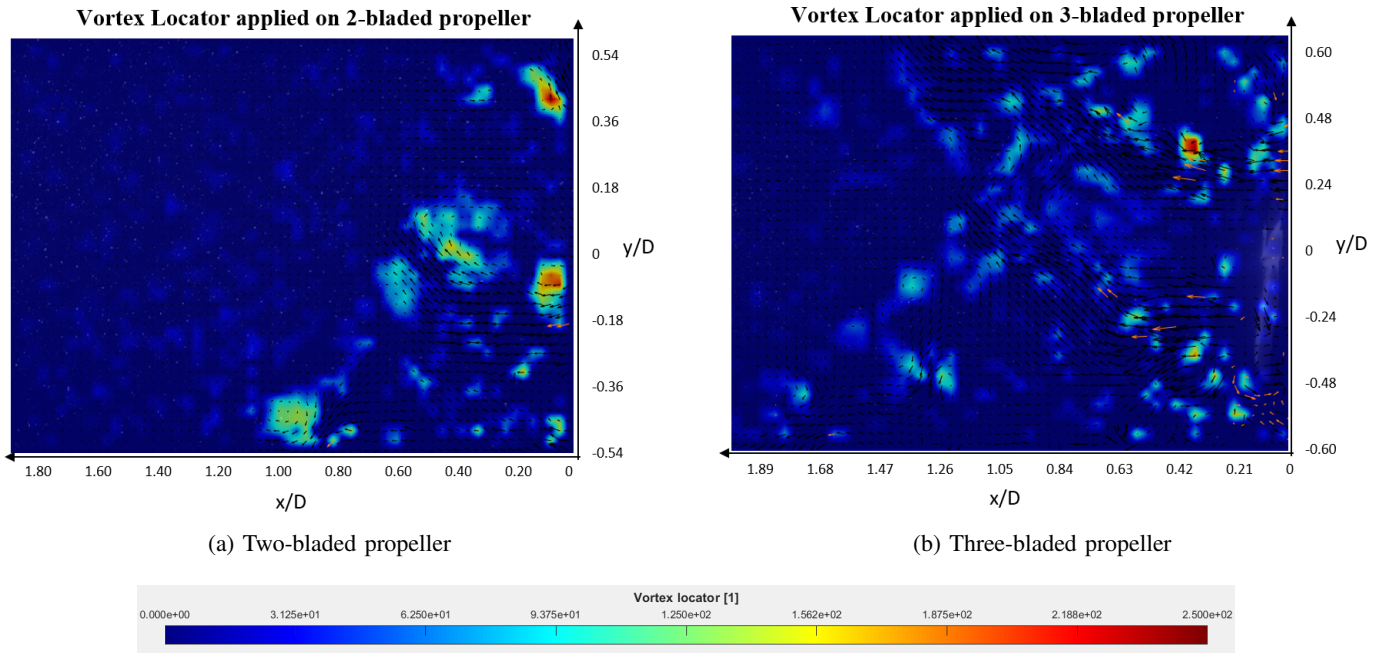

(a) Two-bladed propeller

(b) Three-bladed propeller

(c) Vortex locators on a scale of 0–255

Fig. 3: Vortex locators applied to the velocity field created by two-bladed and three-bladed propellers rotating at 90 RPM.

hub, increasing the likelihood of interaction between tip and hub vortices. These interactions enhance vortex dissipation, which in turn reduces aerodynamic loading on the blades and diminishes tonal noise, contributing to quieter propeller operation—albeit with more complex vortex dynamics.

The dissipation of vortices can be quantified by computing the circulation at two vortex positions - one close to the propeller and the other farther downstream. If there is a dissipation, the maximum circulation at the vortex boundary should be higher for the vortex near the propeller. In Figure 4, the vorticity field is derived from the velocity data of the three-bladed propeller at 120 rpm and the circulation is computed along increasing radial locations starting from the vortex core. The maximum circulation should be at the vortex boundary (marked in red and yellow in the field). Additionally, the circulation becoming a constant for the downstream vortex implies that it is an isolated vortex as can be seen from the vorticity field.

Since most of the studies have been performed on much larger propellers (of diameter more than $250mm$ [9], [3]), it will be worthwhile to investigate some of the challenges faced while studying the velocity field of small propellers, like in the present study where the diameter is just $45mm$. As we increase the rotational speed of the propellers, it becomes very hard to keep track of the evolution of vortices because of the small size of the propellers. The vortices are formed more frequently which increases their mutual interaction and dissipation resulting in multiple smaller structures picked up in vorticity or vortex locator fields.

An example case for both two-bladed and three-bladed propellers rotating at nearly 120 rpm is shown in Figure 5, where the number of vortices was computed using a strict criterion: only those with a vortex generator value above 100 and a lifetime of at least 0.05 seconds were considered vortex centers. Although previous studies suggest that increasing the number of blades generally leads to the formation of more vortices, the present case demonstrates that this relationship is not straightforward. While the three-bladed propeller does show a higher average number of vortices, the results are highly variable over time due to the more rapid dissipation of vortices, making it difficult to generalize.

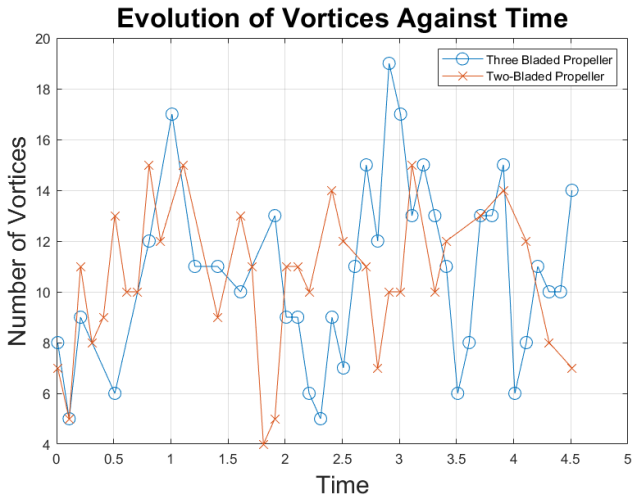

Fig. 5: Tracking the evolution of vortices for two bladed and three bladed propellers at 120 rpm.

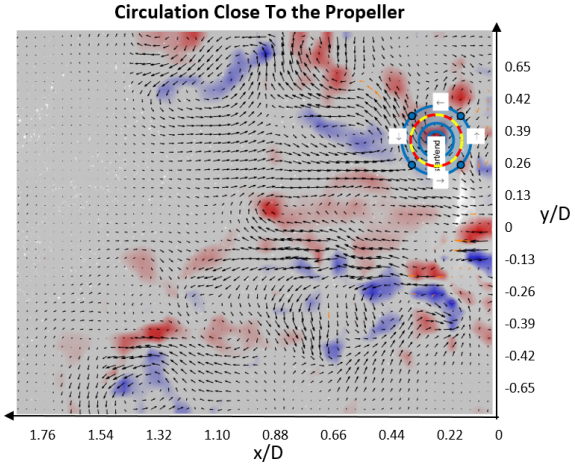

(a) Calculating circulation due to a vortex near the propeller

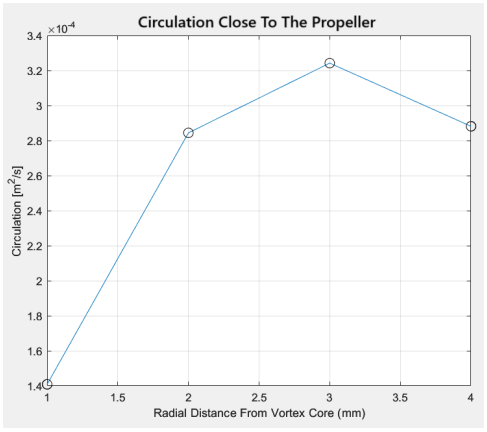

(b) Circulation as a function of increasing radial distance from the vortex core near the propeller

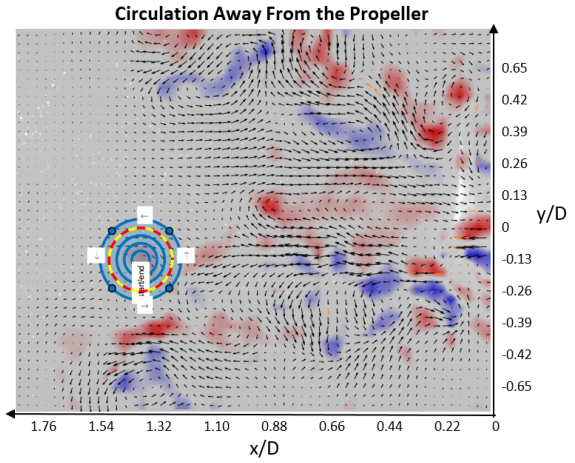

(c) Calculating circulation due to a vortex away from the propeller

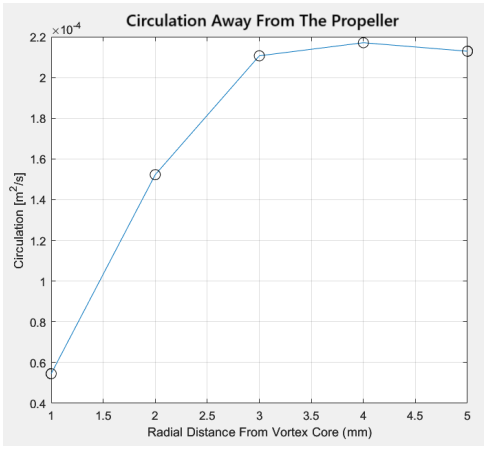

(d) Circulation as a function of increasing radial distance from the vortex core away from the propeller

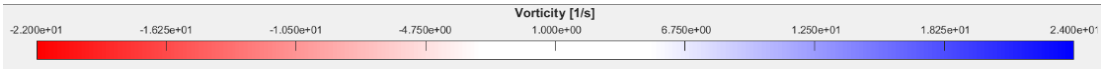

(e) Vortex locator scale (0–255)

Fig. 4: Circulation computed at increasing radial distances at two vortex locations. The vortex boundary is marked in red and yellow where the computed circulation is maximum.

This dilemma can be solved by looking at the vorticity fields in Figure 6, the two-bladed propeller produces prominent vortices that persist and convect almost the entire length of the domain. In contrast, the vortices generated by the three-bladed propeller dissipate more quickly and do not extend to the end of the domain, even though the flow itself reaches that point. This behavior can be attributed to the tendency of larger vortices to break down into smaller structures more rapidly in the three-bladed case, leading to increased dissipation and less persistent vortex structures for the three-bladed case.

An often-overlooked factor influencing vortex dynamics is the limited size of the computational domain. As illustrated in Figure 5, periodic reductions in vortex count are observed, which can be attributed to reverse flow generated by reflection from the downstream boundary. This reversed flow temporarily inhibits vortex formation, likely due to localized adverse pressure gradients [10], though further investigation is needed. The rotating propellers eventually re-establish downstream flow, initiating a repeating cycle of suppression and recovery. This effect becomes more pronounced at higher RPMs, where increased flow velocity leads to shorter intervals between suppression events.

IV. Conclusion

This study investigated the vortex dynamics generated by rotating propellers in quiescent fluid using a desktop Particle Image Velocimetry (PIV) setup. The primary objective was to

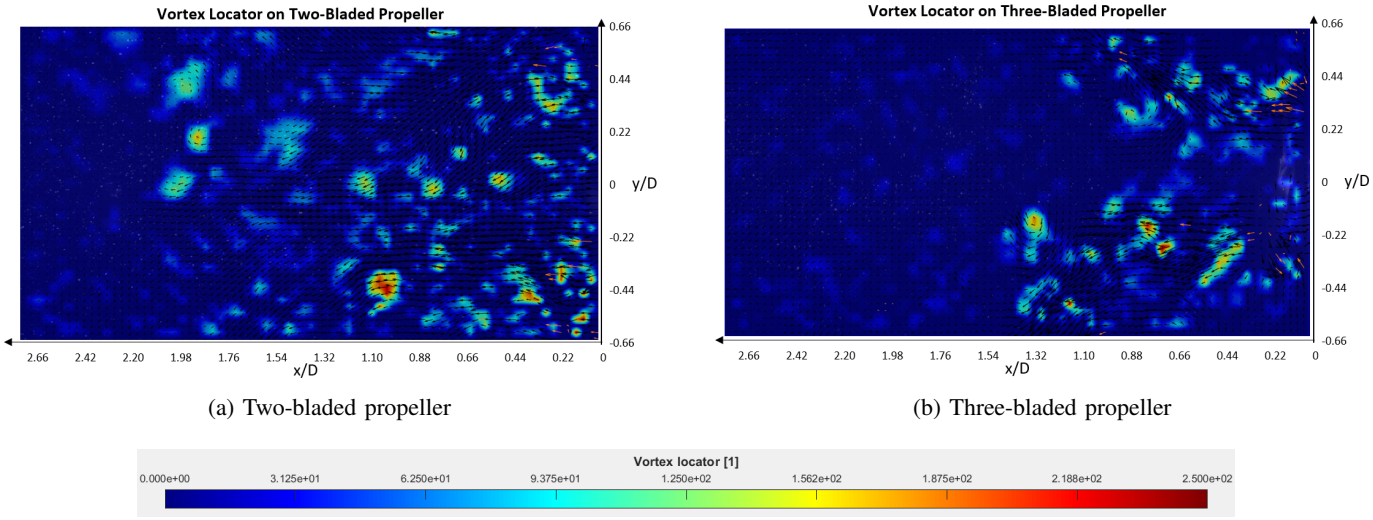

(a) Two-bladed propeller

(b) Three-bladed propeller

(c) Vortex locators on a scale of 0–255

Fig. 6: Vortex locators applied to the velocity field created by two-bladed and three-bladed propellers rotating at 120 RPM.

compare the vortex structures formed by two-bladed and three-bladed propellers of identical diameter. As anticipated, the three-bladed propeller produced greater thrust than the two-bladed counterpart at the same rotational speed.

Among several vortex identification techniques—including vorticity fields, vortex locators, shear rate, and strain rate—the vortex locator method was used as it can directly predict vortex centers. The two-bladed propeller exhibited more distinct and spatially separated vortices that lasted longer in the flow field. Circulation computed from the vorticity field confirmed the progressive weakening of vortices as they convected downstream, attributed to viscous dissipation.

To assess vortex behavior quantitatively, the number of vortices was estimated by applying thresholding criteria to the vortex locator field at 120 RPM. The temporal variation in vortex count revealed cycles of generation and dissipation, with higher counts corresponding to vortex formation and lower counts indicating dominant dissipation. Additionally, reverse flow induced by reflection from the end wall was found to intermittently suppress vortex formation—an effect that became more pronounced at higher RPMs.

The broader aim of this study was to investigate the link between blade count and propeller noise. Since tip vortices are a primary contributor to propeller noise, the observed rapid dissipation of vortices from the three-bladed propeller suggest a mechanism for quieter operation. However, further investigations have to be performed to comment on additional factors affecting propeller noise. These findings offer valuable insights for the development of low-noise propeller designs in aerospace and marine applications.

Acknowledgment

I am profoundly grateful to my parents for their unwavering love and encouragement throughout my academic journey. I extend my heartfelt appreciation to my course instructor, Prof. Kiran Raj M, whose guidance and support have been invaluable in navigating through this project. I express my sincerest gratitude to Mr. Rafe Ali, the course Teaching Assistant, whose sincere efforts helped me perform the experiments in a timely manner.

References

[1] B.-G. Paik, J. Kim, Y.-H. Park, K.-S. Kim, and K.-K. Yu, "Analysis of wake behind a rotating propeller using piv technique in a cavitation tunnel," *Ocean Engineering*, vol. 34, no. 3-4, pp. 594–604, March-April 2007.

[2] K. Baskaran, N. S. Jamaluddin, A. Celik, D. Rezgui, and M. Azarpeyvand, "Effects of number of blades on propeller noise," *Journal of Sound and Vibration*, vol. 572, p. 118176, March 2024.

[3] A. Cotroni, F. D. Felice, G. P. Romano, and M. Elefante, "Investigation of the near wake of a propeller using particle image velocimetry," *Experiments in Fluids*, vol. Suppl., pp. S227–S236, 2000.

[4] R. Soto-Valle, S. Cioni, S. Bartholmay, M. Manolesos, C. N. Nayeri, A. Bianchini, and C. O. Paschereit, "Vortex identification methods applied to wind turbine tip vortices," *Wind Energy Science*, vol. 7, no. 2, pp. 585–602, 2022. [Online]. Available: https://doi.org/10.5194/wes-7-585-2022

[5] W. Thielicke and E. J. Stamhuis, "Pivlab – towards user-friendly, affordable and accurate digital particle image velocimetry in matlab," *Journal of Open Research Software*, vol. 2, no. 1, p. e30, 2014.

[6] W. Thielicke and R. Sonntag, "Particle image velocimetry for matlab: Accuracy and enhanced algorithms in pivlab," *Journal of Open Research Software*, vol. 9, p. 12, 2021.

[7] H.-D. Yao, Z. Huang, L. Davidson, J. Niu, and Z.-W. Chen, "Blade-tip vortex noise mitigation traded-off against aerodynamic design for propellers of future electric aircraft," *Aerospace*, vol. 9, no. 12, p. 825, 2022.

[8] E. J. Stamhuis, "Basics and principles of particle image velocimetry (piv) for mapping biogenic and biologically relevant flows," *Aquatic Ecology*, vol. 40, no. 4, pp. 463–479, 2006.

[9] S. Grizzi, M. Falchi, E. Martellini, G. Aloisio, and T. Pagliaroli, "Piv wake survey of a drone propeller for amphibious applications," in *Journal of Physics: Conference Series, AIVELA XXX National Meeting*, vol. 2590. Rome, Italy: IOP Publishing, 2023, p. 012010.

[10] D. Pagan and R. Benay, "Vortex breakdown induced by an adverse pressure gradient: Experimental and numerical approaches," in *5th Applied Aerodynamics Conference*. Monterey, CA, USA: AIAA, 1987, published online: 17 Aug 2012. [Online]. Available: https://doi.org/10.2514/6.1987-2478